

On de-Sitter Geometry in Cosmic Void Statistics

G. W. Gibbons¹, M. C. Werner^{2,4*}, N. Yoshida^{2,3} and S. Chon³

¹*Department of Applied Mathematics and Theoretical Physics, University of Cambridge, Wilberforce Road, Cambridge, CB3 0WA, UK*

²*Kavli Institute for the Physics and Mathematics of the Universe (WPI), University of Tokyo, 5-1-5 Kashiwanoha, Kashiwa, 277-8583, Japan,*

³*Department of Physics, University of Tokyo, 7-3-1 Hongo, Tokyo, 113-0033, Japan,*

⁴*Department of Mathematics, Duke University, Durham, NC 27708, USA*

This draft 26 August 2013

ABSTRACT

Starting from the geometrical concept of a 4-dimensional de-Sitter configuration of spheres in Euclidean 3-space and modelling voids in the Universe as spheres, we show that a uniform distribution over this configuration space implies a power-law for the void number density which is consistent with results from the excursion set formalism and from data, for an intermediate range of void volumes. We also discuss the effect of restricting the survey geometry on the void statistics. This work is a new application of de-Sitter geometry to cosmology and also provides a new geometrical perspective on self-similarity in cosmology.

Key words: cosmology:theory–large-scale structure of Universe

1 INTRODUCTION

While the existence and characteristic distributions of empty regions are already implicit in early self-similar models of structure hierarchy in the Universe (cf. Mandelbrot (1977)), it was the observational discovery of large, approximately spherical regions almost devoid of visible galaxies known as voids and supervoids (e.g., Kirshner et al. (1981)) that sparked further theoretical work on underdense regions in the Universe. This included analytical studies of the dynamical evolution of individual voids and shell-crossing (Peebles (1982); Sato (1982)) as well as statistical properties of the void distribution. Applying a simple sign-reversal argument, Icke (1984) pointed out that the sphericity of underdense regions increases due to gravitational dynamics, so that it is in fact natural to expect approximately spherical voids. Early theoretical approaches to void statistics used Poisson statistics of empty regions, as developed by Politzer & Preskill (1986), Voronoi tessellations (Icke & van de Weygaert (1987)), and structure formation theory in analogy to the statistics of overdensity peaks (Bardeen et al. (1986)) in Gaussian primordial density fluctuations (e.g., Betancourt-Rijo (1990)). Self-similar features in the void size distribution were also noted (e.g., Einasto, Einasto & Gramann (1989)). Of course, much of this earlier work concentrated on Einstein-de-Sitter cosmology with $\Omega_M = 1$, as was favoured then. Especially after the discovery of the near-isotropic CMB, it was realized that the largest observable voids were difficult to explain theoretically and may therefore provide important cosmological constraints (e.g., Blumenthal et al. (1992)). Attention has also been drawn to galaxy properties within voids (e.g., the void phenomenon of Peebles (2001)). Now, with the advent of the Λ CDM paradigm, detailed numerical studies of void statistics (e.g., Colberg et al. (2005) for a comparison) and

analytical studies of void shape evolution in redshift space (e.g., Maeda, Sakai & Triay (2011)) have been conducted. Moreover, the void formation theory based on the excursion set formalism of primordial density fluctuations has been refined to include the notion of hierarchy (Sheth & van de Weygaert (2004)). This formalism was extended more recently to investigate effects of non-Gaussianity (e.g., D’Amico et al. (2011)) and modified theories of gravity (e.g., Clampitt, Cai & Li (2013)) on voids. Following earlier work on self-similarity, Gaité (2009) applied advanced fractal structures to void statistics. On the observational side, a void catalogue extracted from the SDSS Data Release 7 has recently been published (Pan et al. (2012)), which illustrates the strong dependence of void statistics on the underlying void definition. The possibility of using voids for precision cosmology has also been explored (e.g., Lavaux & Wandelt (2010)). A fitting formula which matches the distributions of voids extracted from 2dF Galaxy Redshift Survey observations and from the Millennium Simulation has been proposed by von Benda-Beckmann & Müller (2008), who also discussed self-similarity in the void size distribution. Higuchi, Oguri & Hamana (2013) have shown how weak lensing observations may be used to measure the mass distribution of voids.

In this paper, we propose a new geometrical approach to void statistics based on the idea that voids can be modelled well by spheres in the Euclidean 3-space. Each such sphere is represented by a point in the 4-dimensional configuration space of spheres, with radius and centre position as coordinates. Since the spatial contact between these spheres is physically important (e.g., in the evolution of voids), it is interesting to consider transformations of the configuration space that preserve such contact relations, namely conformal transformations, in order to define a distance measure on the configuration space. Given these assumptions, it turns out that the configuration space has a de-Sitter geometry, with timelike radii and spacelike centre positions of the spheres, which emerges from

* E-mail:marcus.werner@ipmu.jp

classical sphere geometry and is different from cosmological de-Sitter spacetime. One can now study the size distribution of spherical voids in the Universe in terms of their distribution over this de-Sitter configuration space. The approach presented here has been inspired by other notions of configuration space measures in cosmology (e.g., Gibbons & Turok (2008)), and another application of this de-Sitter configuration space of spheres in a different astronomical context has been proposed recently (Gibbons & Werner (2013)).

The outline of this work is as follows. In Section 2, we give a brief review of the de-Sitter configuration space for the general case of n -spheres in $n + 1$ -dimensional Euclidean space and indicate its conformal structure. This is followed by a discussion of a uniform distribution over the 4-dimensional de-Sitter configuration space used to model voids, that is $n = 2$, in Section 3. We shall derive, firstly, the corresponding void size distribution for voids in the whole (unrestricted) 3-space and find a self-similar power-law. Secondly, the effect of restricting void positions in 3-space due to survey geometry is studied, which naturally breaks the self-similarity of the size distribution. This is carried out analytically for a survey volume shaped as a spherical sector. Then in Section 4, we investigate how the void size distributions predicted by the unrestricted and restricted uniform de-Sitter distributions compare with actual void size distributions. We consider, firstly, theoretical models of self-similarity and the excursion set formalism, to find that the power-law from the unrestricted uniform distribution is, to an extent, consistent with the expectation from structure formation theory. To illustrate this and the effect of survey geometry restriction in a data set, we apply an N-body simulation using the GADGET2 (Springel (2005)) code and extract spherical voids. A comparison with the fitting formula of von Benda-Beckmann & Müller (2008) is also given. Section 5 contains our conclusions and comments on possible further applications of this idea.

2 DE-SITTER CONFIGURATION SPACE

We begin by briefly recapitulating the notion of a configuration space of spheres in Euclidean space and its de-Sitter geometry, as discussed in some more detail in Gibbons & Werner (2013); see also Zee (2013). Consider an n -dimensional unoriented sphere $\mathbb{S}^n(R, \mathbf{x})$ in $n + 1$ -dimensional Euclidean space \mathbb{E}^{n+1} given in terms of its radius $R > 0$ and its centre at $\mathbf{x} = (x^1, \dots, x^{n+1}) \in \mathbb{E}^{n+1}$. It turns out that, to each such sphere, one can uniquely assign a point $X^\mu = (X^0, \mathbf{X}, X^{n+2})$, $0 \leq \mu \leq n + 2$, in $n + 3$ -dimensional Minkowski space $\mathbb{E}^{1, n+2}$ endowed with the usual metric $\eta_{\mu\nu} = \text{diag}(-1, 1, \dots, 1)$, with

$$\begin{aligned} X^0 &= -\frac{1}{2} \left(\frac{\mathbf{x}^2 - 1}{R} - R \right), \\ \mathbf{X} &= -\frac{\mathbf{x}}{R}, \\ X^{n+2} &= -\frac{1}{2} \left(\frac{\mathbf{x}^2 + 1}{R} - R \right), \end{aligned}$$

on the $n + 2$ -dimensional hypersurface

$$\eta_{\mu\nu} X^\mu X^\nu = 1,$$

which is a de-Sitter quadric. In other words, each sphere with a given centre and radius corresponds to a point on an $n + 2$ -dimensional de-Sitter space dS^{n+2} which can therefore be interpreted as a configuration space of spheres. Since for unoriented spheres one may set $R > 0$, we have $X^0 - X^{n+2} = \frac{1}{R} > 0$.

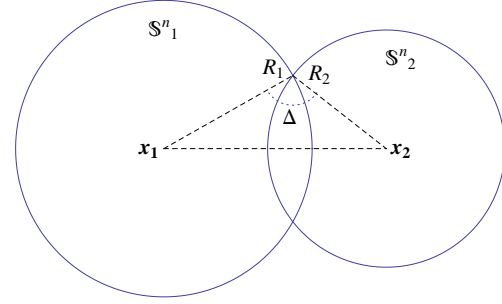


Figure 1. Angle between spheres. The intersection of two n -spheres $\mathbb{S}_1^n(R_1, \mathbf{x}_1), \mathbb{S}_2^n(R_2, \mathbf{x}_2)$ in \mathbb{E}^{n+1} , here illustrated for the case $n = 1$ and, in projection, $n = 2$, can be characterized by the Euclidean angle $\Delta(\mathbb{S}_1^n, \mathbb{S}_2^n)$ given in eq. (3), which is an invariant of the isometries of the de-Sitter configuration space.

Therefore, the space of unoriented spheres is in fact given by half of the full de-Sitter quadric, sometimes referred to as de-Sitter space modulo the antipodal map $X^\mu \mapsto -X^\mu$. Geometrically, the coordinates X^μ of a sphere can be regarded as a form of Lie cycle coordinates for the Laguerre cycle representing the sphere (see, e.g., the appendix of Gibbons & Werner (2013) for more mathematical details). Taking $y^i = (R, \mathbf{x})$, $0 \leq i \leq n + 1$, as coordinates of the de-Sitter configuration space, its metric g induced by the ambient Minkowski metric in the usual way can be read off from the line element

$$\begin{aligned} ds^2 &= \left(-(dX^0)^2 + (d\mathbf{X})^2 + (dX^{n+2})^2 \right) |_{dS^{n+2}} \\ &= \frac{1}{R^2} (-dR^2 + d\mathbf{x}^2) \\ &= g_{ij} dy^i dy^j \end{aligned} \quad (1)$$

so that, with respect to the coordinate-induced basis,

$$g_{ij} = \text{diag} \left(-\frac{1}{R^2}, \frac{1}{R^2}, \dots, \frac{1}{R^2} \right). \quad (2)$$

Hence, this metric measures the distance between spheres in terms of their configuration, that is, their radii and positions in space. Isometries of this de-Sitter space can be identified with conformal transformations of spheres, for the following reason. Consider two intersecting spheres $\mathbb{S}_1^n(R_1, \mathbf{x}_1)$ and $\mathbb{S}_2^n(R_2, \mathbf{x}_2)$ given by X_1^μ and X_2^μ , respectively. Then

$$\begin{aligned} (\eta_{\mu\nu} X_1^\mu X_2^\nu) |_{dS^{n+2}} &= \frac{R_1^2 + R_2^2 - (\mathbf{x}_1 - \mathbf{x}_2)^2}{2R_1 R_2} \\ &= \cos \Delta(\mathbb{S}_1^n, \mathbb{S}_2^n), \end{aligned} \quad (3)$$

so that isometries leave the Euclidean angle $\Delta(\mathbb{S}_1^n, \mathbb{S}_2^n)$ between the two spheres invariant which, as illustrated in Fig. 1, measures their contact. Indeed, it provides a geometrical interpretation for the line element (1), since for two spheres that are infinitesimally close in the configuration space so that they are nearly identical in their radii and positions, one finds,

$$\begin{aligned} ds^2 &= \frac{1}{R^2} (-dR^2 + d\mathbf{x}^2) \\ &= d\Delta^2(\mathbb{S}^n(R, \mathbf{x}), \mathbb{S}^n(R + dR, \mathbf{x} + d\mathbf{x})). \end{aligned}$$

Finally, a measure of the number of spheres having radii within $[R, R + dR]$ and centres in the volume element $dx^1 \dots dx^{n+1}$ at $\mathbf{x} \in \mathbb{E}^{n+1}$ is provided by the volume element,

$$dV^{n+2} = \sqrt{-\det g_{ij}} dy^0 \dots dy^{n+1}$$

$$= \frac{1}{R^{n+2}} dR dx^1 \dots dx^{n+1}, \quad (4)$$

of the $n + 2$ -dimensional de-Sitter configuration space.

3 UNIFORM DISTRIBUTION OVER dS^4

3.1 Without survey geometry restriction

In order to study the distribution of cosmic voids from the geometrical perspective of the de-Sitter configuration space, we shall model them as unoriented 2-spheres in \mathbb{E}^3 . Hence specializing the previous discussion to the case $n = 2$, the corresponding 4-dimensional configuration space has the de-Sitter geometry dS^4 with metric given by (2). Then the configuration space volume element for voids with radii in $[R, R + dR]$ and with centres in the volume element $dx^1 dx^2 dx^3$ at $\mathbf{x} \in \mathbb{E}^3$ becomes

$$dV^4 = \frac{1}{R^4} dR dx^1 dx^2 dx^3, \quad (5)$$

from eq. (4). Also, the infinitesimal number of voids dN with radii in $[R, R + dR]$ centred within the volume element at \mathbf{x} can be described in terms of a non-negative distribution function over the configuration space, $f : dS^4 \rightarrow \mathbb{R}^+$, so that

$$dN = f(R, \mathbf{x}) dR dx^1 dx^2 dx^3. \quad (6)$$

In this section, we will consider the simplest distribution in this framework, corresponding to a uniform distribution of voids over the de-Sitter configuration space such that

$$dN \propto dV^4.$$

Clearly, this uniform distribution has the property that all voids are counted regardless of their position in \mathbb{E}^3 : there is no restriction due to survey geometry and any mutual overlap of voids that may occur is ignored. The corresponding distribution function f is independent of the position in space,

$$f(R, \mathbf{x}) \propto \frac{1}{R^4}, \quad (7)$$

from eq. (5) and (6). Defining the void number density as the number of void centres per volume element in \mathbb{E}^3 , one can compute the cumulative number density $n(> R)$ of voids with radius greater than R that corresponds to the uniform distribution,

$$n(> R) = \int_R^\infty f(R') dR' \propto \frac{1}{R^3},$$

by integrating (6) using (7). Expressing this in terms of void volume $V = 4\pi R^3/3$,

$$n(> V) \propto \frac{1}{\sqrt{V}}. \quad (8)$$

A more realistic modification of this cumulative number density should take into account that any actual void survey can, of course, only encompass a finite subregion of \mathbb{E}^3 . We shall investigate this in the following.

3.2 With survey geometry restriction

The assumption of a uniform distribution of voids over their de-Sitter configuration space results in a differential number density

$$\frac{dn}{dR} = f(R) \propto \frac{1}{R^4} \Rightarrow \frac{dn}{dV} = \frac{dR}{dV} \frac{dn}{dR} \propto \frac{1}{V^2} \quad (9)$$

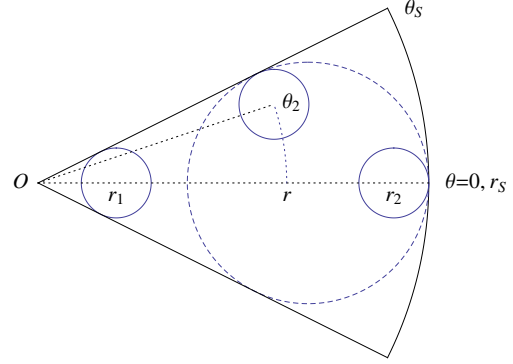


Figure 2. Survey geometry. In a survey region shaped as spherical sector with $r \leq r_S$, $\theta \leq \theta_S$ centred at the observer O , the limits $r_1(R)$, $r_2(R)$ and $\theta_2(r, R)$ for voids of radius R (solid circles) are illustrated, see eq.s (10). The largest void for the given survey geometry, at r_0 with radius R_0 given by eq. (11), is also shown (dashed circle).

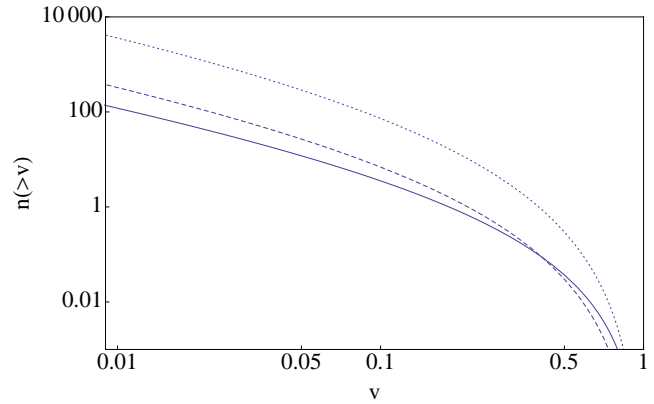


Figure 3. Cumulative number density of voids. Double logarithmic plots of $n(> v)$, the integral (15) with the same constant of proportionality and r_S set to unity, as functions of the dimensionless volume parameter $0 \leq v \leq 1$ defined in (12), for three choices of the opening angle θ_S of the survey geometry: a solid curve for $\theta_S = \pi/2$, the half sphere; a dashed curve for $\theta_S = \pi/6$; and a dotted curve for $\theta_S = \pi/18$.

of dn void centres per volume in \mathbb{E}^3 , per void radius dR or void volume dV , respectively, again by eq. (6) and (7). Now suppose that a survey counts only those voids which are wholly within the survey region V_S . For simplicity, consider a survey geometry shaped as a spherical sector with opening angle θ_S and maximal (comoving) distance r_S from an observer who is situated at its apex and coordinate origin. Then, in terms of spherical polar coordinates, the survey region can be described by

$$V_S : 0 \leq r \leq r_S, \quad 0 \leq \theta \leq \theta_S, \quad 0 \leq \phi \leq 2\pi,$$

and we let $\theta_S \leq \pi/2$. The total volume of the survey is then

$$V_S(r_S, \theta_S) = \frac{2\pi}{3} r_S^3 (1 - \cos \theta_S).$$

A given void of radius R will be counted in the distribution if it lies wholly within V_S , that is, if the coordinates of its centre (r, θ, ϕ) satisfy the conditions

$$V_S(R) : r_1(R) \leq r \leq r_2(R), \quad 0 \leq \theta \leq \theta_2(r, R), \quad 0 \leq \phi \leq 2\pi,$$

where the lower and upper coordinate limits are determined by voids touching the boundary of V_S . The conditions for these can be read off from Fig. 2,

$$r_1(R) \sin \theta_S = R, \quad r_2(R) + R = r_S, \quad r \sin(\theta_S - \theta_2(r, R)) = R,$$

whence we have

$$\begin{aligned} r_1(R) &= \frac{R}{\sin \theta_S}, \\ r_2(R) &= r_S - R, \\ \theta_2(r, R) &= \theta_S - \arcsin \frac{R}{r}. \end{aligned} \quad (10)$$

The largest void which fits into V_S is situated at r_0 on the polar axis and has radius R_0 , whose values can be obtained from the condition $r_1(R_0) = r_2(R_0)$. Hence, using eq. (10),

$$r_0 = \frac{r_S}{1 + \sin \theta_S}, \quad R_0 = \frac{r_S \sin \theta_S}{1 + \sin \theta_S}. \quad (11)$$

In order to compare different survey geometries, it will be convenient to express void volume V in terms of the volume V_0 of the largest void admitted by a given survey geometry (r_S, θ_S) , and hence define the dimensionless quantity $0 \leq v \leq 1$,

$$v = \frac{V}{V_0(r_S, \theta_S)} \quad \text{such that} \quad R = \frac{r_S \sin \theta_S}{1 + \sin \theta_S} v^{\frac{1}{3}} \quad (12)$$

from eq. (11). The differential number density of voids within the range $[v, v + dv]$ of the volume parameter can then be expressed as

$$dn = \frac{1}{V_S(r_S, \theta_S)} \int_{V_S(v)} dN,$$

so that by eq. (6) in spherical polar coordinates,

$$\frac{dn}{dv} = \frac{1}{V_S(r_S, \theta_S)} \frac{dR}{dv} \int_{V_S(v)} f(v, r, \theta, \phi) r^2 \sin \theta dr d\theta d\phi. \quad (13)$$

Using the limits of $V_S(v)$ for voids with volume parameter v given by (10) and the uniform distribution (7), whose constant of proportionality is kept, we can recast (13) to obtain

$$\begin{aligned} \frac{dn}{dv} &\propto \frac{(1 + \sin \theta_S)^3}{\sin^3 \theta_S (1 - \cos \theta_S) r_S^6 v^2} \int_{r_1}^{r_2} \int_0^{\theta_2} r^2 \sin \theta d\theta dr \\ &= \frac{(1 + \sin \theta_S)^3}{3 \sin^3 \theta_S (1 - \cos \theta_S) r_S^3 v^2} \left[1 \right. \\ &\quad \left. - \frac{3 \sin \theta_S (2 + \sin \theta_S)}{2 (1 + \sin \theta_S)} v^{\frac{1}{3}} + \frac{\sin^2 \theta_S}{1 + \sin \theta_S} \left(3v^{\frac{2}{3}} - \frac{v}{2} \right) \right. \\ &\quad \left. - \cos \theta_S \left(1 - \frac{2 \sin \theta_S}{1 + \sin \theta_S} v^{\frac{1}{3}} \right)^{\frac{3}{2}} \right]. \end{aligned} \quad (14)$$

This expression can in turn be integrated to yield the corresponding cumulative number density,

$$n(> v) = \int_v^1 \frac{dn}{dv'} dv', \quad (15)$$

and Fig. 3 shows it for three choices of the opening angle θ_S of the survey geometry. These results for the number density (14) and cumulative number density of voids illustrate how the intrinsic distribution and the observed distribution can differ substantially due to the restrictions imposed by the survey geometry. Small voids, of course, tend to be affected less by the survey geometry and therefore approach asymptotically the power-law (8) of the intrinsic distribution.

4 COMPARISON WITH VOID DISTRIBUTIONS

4.1 From theoretical models

4.1.1 Self-similarity

As shown in Section 3.1, the uniform de-Sitter distribution without survey geometry restriction yields a power-law size distribution given by

$$\nu(V) := \frac{dn}{dV} \propto \frac{1}{V^2} \quad (16)$$

for the differential number density of voids, from eq. (9). This is obviously self-similar in the sense that a change in volume scale, $\tilde{V} = sV$, $s = \text{const.}$, also implies

$$\nu(\tilde{V}) \propto \frac{1}{\tilde{V}^2}.$$

Moreover, since, for a given volume in \mathbb{E}^3 , the integer rank \mathcal{R} of a void in an ordered sequence decreasing in size from largest one is proportional to $n(> V)$, one can see from (8) that Zipf's law is satisfied. The applicability of fractal structures and Zipf's law to void distributions was investigated in detail by Gaite & Manrubia (2002), showing that, in our notation for a void of volume V in \mathbb{E}^3 ,

$$V(\mathcal{R}) \propto \mathcal{R}^{-\frac{3}{D}},$$

where $D < 3$ is the fractal dimension, so that in terms of the cumulative number density with $\mathcal{R} \propto n(> V)$,

$$n(> V) \propto V^{-\frac{D}{3}}.$$

Hence, the inverse power-law of eq. (8) represents a limiting case that cannot be described by a fractal set with one dimension $D < 3$. In fact, Gaite (2007) shows that the extended notion of a multifractal, a set with multiple fractal dimensions, is useful in this context (see also Gaite (2009); a recent review on scaling laws in the large scale structure more generally is given by Jones et al. (2004)). Of course, the property of self-similarity does not fix the power in (16) by itself, which will depend on the underlying physics. It is therefore interesting to note that the self-similar power-law (16) from the uniform de-Sitter distribution has also been found to arise in the excursion set formalism of structure formation, as we shall outline below.

4.1.2 Excursion set formalism

In their pioneering paper, Press & Schechter (1974) point out that, starting from Gaussian density perturbations in a Friedmann cosmology and considering the linear quasi-Newtonian perturbation analysis of the growing mode, the mass distribution at late times does not depend on the initial mass distribution. They identify a simple physical reason for this self-similarity in the existence of two dimensionless quantities governing the gravitational collapse, which remain approximately *constant* during the matter-dominated phase on subhorizon scales. The Press-Schechter argument yielding a power-law size distribution can be summarized as follows. Consider massive particles distributed in some comoving volume. Then the mass density function ρ on this volume is obtained by applying some smoothing window function with scale length l at each point. At sufficiently early times, this density function will be approximately constant,

$$\rho = \bar{\rho}(1 + \delta), \quad |\delta| \ll 1.$$

However, if the density within a window is greater than some (fixed dimensionless, say) critical density so that $\delta > \delta_{\text{crit}}$ around overdensity peaks due to fluctuations in the density function, then the mass within the window will gravitationally collapse and ultimately form a bound object. Again, for sufficiently early times, one may take these fluctuations to be Gaussian, such that the volume fraction of points with collapsing windows is given by

$$\mathcal{F} \propto \frac{1}{\sigma} \int_{\delta_{\text{crit}}}^{\infty} \exp\left(-\frac{\delta}{2\sigma^2}\right) d\delta.$$

These windows will contain slightly different masses, but basically $M \propto \bar{\rho} l^3$. Also, the variance may depend on the smoothing scale and hence also on the mass, $\sigma^2 \propto l^{-n-3} \propto M^{-n/3-1}$, for some spectral index $n \geq -3$. Thus, \mathcal{F} is a function M as well, and so the differential number density $\nu(M)$ of ultimately bound objects obeys

$$M\nu(M) \propto -\bar{\rho} \frac{d\mathcal{F}}{dM} = -\bar{\rho} \frac{d\sigma}{dM} \frac{d\mathcal{F}}{d\sigma}, \quad (17)$$

and hence

$$\nu(M) \propto M^{-\frac{n}{6} - \frac{3}{2}} \quad \text{for } M \ll M_0,$$

where M_0 is the mass scale of the exponential term, which gives rise to a cutoff at large masses (or volumes). For a scale-invariant σ , that is $n = -3$, this yields the inverse square power-law

$$\nu(M) \propto M^{-2}. \quad (18)$$

It turns out that this power-law emerges also in the modified Press-Schechter approach proposed by Appel & Jones (1990), which uses an adaptive window scale l . Now in the context of voids, one can consider underdensity troughs rather than overdensity peaks (as in Bardeen et al. (1986)) and, since Gaussian fluctuations are symmetric about the average density, the same power-law applies, as pointed out by Sheth & van de Weygaert (2004). Then since $M \propto l^3 \propto V$, we recover (16) from (18). Of course, in addition to the large volume cutoff, this simple excursion set argument ignores effects of void hierarchy which affect small volumes in particular (i.e., by the void-in-void and void-in-cloud processes, cf. Sheth & van de Weygaert (2004)), so that the power-law will only apply within a range of volumes.

Hence, at least within a range of volumes, the power-law (16) has a physical basis in the excursion set formalism: the Gaussian fluctuations producing voids give rise to a self-similar power-law size distribution which can be described geometrically as a uniform distribution over the de-Sitter configuration space of spheres.

4.2 From data

4.2.1 An N-body simulation

Now in order to compare the void size distributions predicted by the unrestricted and restricted uniform de-Sitter distributions from Section 3 with data, we perform an N-body simulation with the parallel Tree-Particle Mesh code, GADGET2 (Springel (2005)), using cosmological parameters consistent with the WMAP seven-year results (Komatsu et al. (2011)), namely spatial curvature $k = 0$, dark energy density $\Omega_\Lambda = 0.7274$, Hubble parameter $h = 0.704$ and spectral index $n_s = 0.963$. The initial condition for the simulation is generated at redshift $z_0 = 50$ using the code developed by Nishimichi et al. (2009), who employ second order Lagrangian perturbation theory. The simulation is run in a cubic box with side length $240h^{-1}\text{Mpc}$ in comoving coordinates with periodic boundary conditions, and 256^3 dark matter particles whose individual

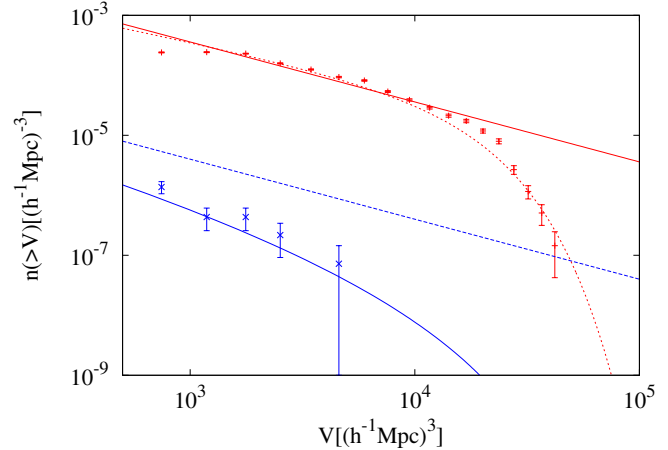


Figure 4. Simulated void size distributions. Double logarithmic plots of the cumulative number density of voids as a function of volume, using the simulation discussed in Section 4.2: uniform de-Sitter distribution from eq. (8) without survey geometry restriction (upper solid curve and data set) and fitting formula of von Benda-Beckmann & Müller (2008) (dotted); uniform de-Sitter distribution from eq. (15) with survey geometry restriction in spherical sector (lower solid curve and data set) and corresponding power-law asymptote (dashed). Poisson errors are indicated.

mass is scaled to match the mass density of the Universe. At redshift $z = 0$, voids are extracted according to the following algorithm.

Firstly, the discrete simulation data are smoothed to construct the matter density function, using a Gaussian window with adaptive length scale. This smoothing length is chosen to be the distance to the 20th nearest particle at each cell. Secondly, a set of spherical voids is extracted by defining density minima as void centres and determining the radius for each void as the largest radius R centered at the density minimum for which the average density of the enclosed sphere $\rho(R)$ is less than a critical value

$$\delta_{\text{crit}} = \frac{\rho(R) - \bar{\rho}}{\bar{\rho}} = -0.8,$$

relative to the average density $\bar{\rho}$ of the box. Hence, for our present purposes, we ignore the overlap of the spherical voids and do not apply an additional merging algorithm to these voids (cf. Colberg et al. (2005), also called ‘protovoids’), which would give rise to non-spherical voids. This should allow for a meaningful comparison with the uniform distribution over the de-Sitter configuration space of spheres, which allows void overlap as noted in Section 3.1.

4.2.2 Discussion

The resulting cumulative number density of voids in the simulation box as a function of void volume is shown in Fig. 4. The largest void has a volume of $V_{\text{max}} \simeq 4.2 \cdot 10^4 (h^{-1}\text{Mpc})^3$, which can be interpreted in terms of the exponential cutoff in the excursion set formalism mentioned in Section 4.1.2, and whose value is comparable with the simulation results reported in Fig. 7 of Colberg et al. (2005). Until the curve flattens at very small volumes – here, of course, rather due to simulation resolution and smoothing scale than effects of void hierarchy –, the cumulative number density for $V \ll V_{\text{max}}$ can indeed be approximated by the power-law of eq. (8) derived from the unrestricted uniform de-Sitter distribution. It is also instructive to compare this result with the fitting formula of von Benda-Beckmann & Müller (2008), which was shown to

model well the cumulative volume filling factor $F(> R)$ of voids derived from magnitude-limited samples of galaxies in the 2dF Galaxy Redshift Survey,

$$F(> R) = \exp \left[- \left(\frac{R}{s_1 \lambda} \right)^{p_1} - \left(\frac{R}{s_2 \lambda} \right)^{p_2} \right], \quad (19)$$

where $R = (3V/4\pi)^{1/3}$ is the effective spherical radius of a void of volume V and any shape, λ denotes the mean separation between galaxies, and p_1, p_2, s_1, s_2 are parameters. In order to convert this to a cumulative number density as a function of volume, one can rewrite eq. (19) in terms of V . Again ignoring void overlap,

$$F(> V) = \int_V^\infty V' \frac{dn}{dV'} dV',$$

and we have

$$\frac{dn}{dV} = - \frac{1}{V} \frac{dF(> V)}{dV},$$

so that

$$n(> V) = \int_V^\infty \frac{dn}{dV'} dV' = - \int_V^\infty \frac{1}{V'} \frac{dF(> V')}{dV'} dV'$$

can be computed from (19). While a detailed comparison is beyond the scope of this paper, we note that the parameters $p_1 = 1$, $p_2 = 4.5$, $s_1 = 1$, $s_2 = 1.5$ and $\lambda = 11 h^{-1} \text{Mpc}$, which seem appropriate choices given the data in Tables 1 and 2 of von Benda-Beckmann & Müller (2008), yield a curve in reasonable agreement with our simulation data, as seen in Fig. (4), using a factor of 2.5 to correct for the fact that our voids are not merged and therefore have a higher cumulative number density. This factor is also compatible with the void number densities shown in Fig. 6 and Fig. 7 of Colberg et al. (2005).

Given, then, that our simulation appears to produce a realistic size distribution of spherical voids without merging, which does indeed agree with the uniform de-Sitter distribution for voids in the range $10^3 \dots 10^4 (h^{-1} \text{Mpc})^3$, we shall now turn to the effect of restricting the survey geometry. To this end, we select a survey region in the simulation box shaped like a spherical sector as in Fig. 2, with its apex at a corner of the box and its axis oriented along the diagonal. Consider such a spherical sector with an opening angle of $\theta_S = 10^\circ$ and a radius of half the maximum radius within the box, $r_S \simeq 169 h^{-1} \text{Mpc}$. Although such a survey volume has only 1.1% of the total box volume, the volume of the largest void within this survey region is $V_0 \simeq 6.5 \cdot 10^4 (h^{-1} \text{Mpc})^3$, from eq. (11), which is greater than V_{max} . The corresponding cumulative number density is also shown in Fig. 4, together with the theoretical prediction of eq. (15) from the restricted uniform de-Sitter distribution. Since, for voids in the whole box, the unrestricted uniform de-Sitter distribution is a good approximation in the range $10^3 \dots 10^4 (h^{-1} \text{Mpc})^3$ where $v = V/V_0$ is of the order 0.1, we expect from Fig. 3 that the survey geometry restriction causes a significant deviation in this range from the power-law asymptote, which represents the effect of the survey volume restriction alone. Furthermore, since $V_0/V_{\text{max}} \simeq 1.5$, we expect no significant effect of the large volume cutoff. Both expectations are indeed borne out by the data, as can be seen in the figure.

5 CONCLUDING REMARKS

"In parallel with efforts to explain, I think it indispensable to describe clustering, and to mimic reality by purely geometric means."

Mandelbrot (1977), p. 84

In this article, we have considered an application of the 4-dimensional de-Sitter configuration space of 2-spheres in Euclidean 3-space to cosmology. Modelling cosmic voids as spheres and ignoring their overlap, it was shown that a uniform distribution over this configuration space gives rise to a self-similar power-law size distribution of voids. It appears to agree well with data in an intermediate range of void volumes, and this can be understood physically from the excursion set formalism as long as the large volume cutoff and void hierarchy effects at small volumes may be ignored. We have also seen how restrictions of void positions in 3-space due to survey geometry significantly affect the size distribution.

Now in order to refine this approach, one might implement void merging conditions using this configuration space language. Furthermore, since the uniform distribution appears to provide a reasonably good match with actual void distributions of intermediate volume, it may be worthwhile to treat the uniform distribution as a null hypothesis and study the physical interpretation of non-uniform distributions. Then deviations from uniformity will, as we have seen, encode physically interesting effects such as void hierarchy processes or the large volume cutoff, which may be particularly sensitive to the underlying cosmology.

Finally, while de-Sitter geometry plays an important and well-known rôle in cosmological spacetimes, we would like to emphasize the interesting, and perhaps rather surprising, fact that the present application of de-Sitter geometry to cosmology arises in a physically entirely different context. At this stage, our approach is primarily a descriptive device which also offers a novel geometrical interpretation of an aspect of self-similarity in cosmology, in the spirit of the quotation above.

ACKNOWLEDGMENTS

MCW gratefully acknowledges support from the World Premier International Research Center Initiative (WPI Initiative), MEXT, Japan. NY acknowledges financial support from the Japan Society for the Promotion of Science (JSPS) Grant-in-Aid for Scientific Research (25287050).

REFERENCES

- Appel L., Jones B. J. T., 1990, MNRAS, 245, 522
- Bardeen J. M., Bond J. R., Kaiser N., Szalay A. S., 1986, ApJ, 304, 15
- Betancourt-Rijo J., 1990, MNRAS, 246, 608
- Blumenthal G. R., Da Costa N., Goldwirth D. S., Lecar M., Piran T., 1992, ApJ, 388, 234
- Clampitt J., Cai Y.-C., Li B., 2013, MNRAS, 431, 749
- Colberg J. M., Sheth R. K., Diaferio A., Gao L., Yoshida N., 2005, MNRAS, 360, 216
- D'Amico G., Musso M., Noreña J., Paranjape A., 2011, PRD, 83, 023521
- Einasto J., Einasto M., Gramann M., 1989, MNRAS, 238, 155
- Gaite J., 2007, ApJ, 658, 11
- Gaite J., 2009, JCAP, 0911, 004
- Gaite J., Manrubia S. C., 2002, MNRAS, 335, 977
- Gibbons G. W., Turok N., 2008, PRD, 77, 063516
- Gibbons G. W., Werner M. C., 2013, MNRAS, 429, 1045
- Higuchi Y., Oguri M., Hamana T., 2013, MNRAS, 432, 1021
- Icke V., 1984, MNRAS, 206, 1P
- Icke V., van de Weygaert R., 1987, A&A, 184, 16

- Jones B. J. T., Martínez V. J., Saar E., Trimble V., 2004, *Rev. Mod. Phys.*, 76, 1211
- Kirshner R. P., Oemler A. Jr., Schechter P. L., Shectman S. A., 1981, *ApJ*, 248, L57
- Komatsu E., Smith K. M., Dunkley J., Bennett C. L., Gold B., Hinshaw G., Jarosik N., Larson D., Nolte M. R., Page L., Spergel D. N., Halpern M., Hill R. S., Kogut A., Limon M., Meyer S. S., Odegard N., Tucker G. S., Weiland J. L., Wollack E., Wright E. L., 2011, *ApJS*, 192, 18
- Lavaux G., Wandelt B. D., 2010, *MNRAS*, 403, 1392
- Maeda K.-I., Sakai N., Triay R., 2011, *JCAP*, 1108, 026
- Mandelbrot B. B., 1977, *The Fractal Geometry of Nature*, W. H. Freeman, New York
- Nishimichi T., Shirata A., Taruya A., Yahata K., Saito S., Suto Y., Takahashi R., Yoshida N., Matsubara T., Sugiyama N., Kayo I., Jing Y., Yoshikawa K., 2009, *PASJ*, 61, 321
- Pan D. C., Vogeley M. S., Hoyle F., Choi Y.-Y., Park C., 2012, *MNRAS*, 421, 926
- Peebles P. J. E., 1982, *ApJ*, 257, 438
- Peebles P. J. E., 2001, *ApJ*, 557, 495
- Politzer H. D., Preskill J. P., 1986, *PRL*, 56, 99
- Press W. H., Schechter P., 1974, *ApJ*, 187, 425
- Sato H., 1982, *Prog. Theor. Phys.*, 68, 236
- Sheth R. K., van de Weygaert R., 2004, *MNRAS*, 350, 517
- Springel V., 2005, *MNRAS*, 364, 1105
- von Benda-Beckmann A. M., Müller V., 2008, *MNRAS*, 384, 1189
- Zee A., 2013, *Einstein Gravity in a Nutshell*, Princeton University Press, Princeton, pp. 646-647